

A Sensitivity-Enhanced Simulation Approach for Community Climate System Model

Jong G. Kim¹, Elizabeth C. Hunke², and William H. Lipscomb²

¹ MCS Division, Argonne National Laboratory
Argonne, Illinois, U.S.A

² Theoretical Division, Los Alamos National Laboratory
Los Alamos, New Mexico, U.S.A

`jkim@mcs.anl.gov`, `eclare@lanl.gov`, `lipscomb@lanl.gov`

Abstract. A global sea-ice modeling component of the Community Climate System Model was augmented with automatic differentiation (AD) technology. The numerical experiments were run with two problem sets of different grid sizes. Rigid ice regions with high viscous properties cause computational difficulty in the propagation of AD-based derivative computation. Pre-tuning step was required to obtain successful convergence behavior. Various thermodynamic and dynamic parameters were selected for multivariate sensitivity analysis. The major parameters controlling the sea-ice thickness/volume computation were ice and snow densities, albedo parameters, thermal conductivities, and emissivity constant. Especially, the ice and snow albedo parameters are found to have stronger effect during melting seasons. This high seasonal variability of the thermodynamic parameters underlines the importance of the multivariate sensitivity approach in global sea-ice modeling studies.

1 Introduction

The Community Climate System Model (CCSM, see www.cesm.ucar.edu) is a fully-coupled, global climate simulation model developed by NCAR and DOE. It provides the capability to simulate the interconnected Earth's climate systems including the atmosphere, ocean, land, and sea-ice. The parameterization schemes of the CCSM model involve a number of adjustable modeling parameters with different scales of uncertainty. This impedes new parameterization schemes since the entire model must be tuned with each new parameterization scheme. Furthermore, current sensitivity analysis and parameter tuning experiments of the CCSM model are performed by slow and labor-intensive approach: "expert judgement" of a handful of scientists. Against this background, the sensitivity-enhanced CCSM simulation approach for the global sea-ice modeling component, CICE was implemented with the AD method. This AD-based approach allows the derivative-enhanced CICE code to simultaneously compute analytical derivatives in addition to original simulation results.

The modeling outputs of the CICE code are the global sea-ice conditions such as ice thickness, compactness, and horizontal velocity [3]. Thermodynamic, dynamic mass and energy balances coupled with transport equations are used to

derive the CICE modeling formulation. There were many early sensitivity studies to see the impact of parameter changes on simulation results. These include the works of Parkinson and Washington [6], Harder and Fischer [2], and Miller et al. [5]. From these studies, it was concluded that sea-ice modeling parameters are strongly interdependent and an objective computational scheme for tuning modeling parameters is a critical step in improving the sea-ice model development. In this paper, we used the AD source code transformation package TAPENADE [4] developed by the French National Institute for Research in Computer Science and Control (INRIA) to investigate the parameter sensitivities of the CICE model. This study was intended to help climate modelers objectively identify important modeling parameters and further use the AD-computed sensitivities as parameter tuning guide. Following a brief discussion of the model and the TAPENADE-based implementation, we discuss the numerical experiments and conclude with a brief summary.

2 Model Description

The major components of the CICE model are the thermodynamics, dynamics, and horizontal transport routines, solving the snow and ice physical status. The governing equations for each modeling component are solved on a generalized orthogonal grid by using an explicit time-step procedure. We summarize the main elements of the formulation here to identify the parameters used in the numerical sensitivity experiments. A complete description can be found in the user's manual of the CICE model [3]. Selected parameters for the sensitivity study are listed in Table 1.

2.1 Thermodynamic Parameters

The thermodynamic portion of the model determines the temperature profile and thickness changes of ice and snow based on an energy balance of radiative, turbulent, and conductive heat fluxes in each grid cell. For the energy flux from the atmosphere to the ice, the incoming shortwave flux is computed as function of α , the shortwave albedo, and i_o , the fraction of absorbed shortwave flux penetrating into the ice. Outgoing longwave radiation takes the standard blackbody form, $F_{L\uparrow} = -\epsilon\sigma(T_{sf})^4$, where ϵ is the emissivity of snow or ice, σ is the Stefan-Boltzmann constant, and T_{sf} is the surface temperature. The minimum wind speed parameter, u_{min} , is used to maintain finite sensible and latent heat fluxes for the situation of no wind. The net absorbed shortwave flux is actually a summation over two different radiative quantities (visible and near-infrared) with two corresponding albedos. In addition to these parameters, the constants such as snow area fraction f_{snow} , penetrating fraction of visible solar radiation i_c , and bulk extinction coefficient κ_i are identified as adjustable to compute the flux of shortwave radiation. The rate of temperature change in the ice interior is computed by the conductive heat balance equation given as a function of various parameters. These include the densities and thermal conductivities of snow and ice. The thermal conductivity is the function of the conductivity of fresh ice k_o ,

Table 1. Model parameters chosen for sensitivity testing

Parameter	Description	Value
ϵ	emissivity of snow and ice	0.95
u_{min}	minimum wind speed for turbulent fluxes	1 m/s
α_{iv}	visible ice albedo	0.78
α_{in}	near-IR ice albedo	0.36
α_{sv}	visible cold snow albedo	0.98
α_{sn}	near-IR snow albedo	0.70
i_c	penetrating fraction of visible solar radiation	0.7
κ_i	visible extinction coefficient in ice	1.4 m^{-1}
ρ_i	ice density	917 kg/m^3
β	T, S proportionality constant in conductivity	0.13 W/m/psu
k_o	thermal conductivity of fresh ice	2.03 W/m/deg
ρ_s	snow density	330 kg/m^3
k_s	thermal conductivity of snow	0.30 W/m/deg
S_{max}	maximum salinity, at ice base	3.2 psu
h_{mix}	ocean mixed-layer depth	20 m
D_w	drag parameter for water on ice	5.49936 kg/m^3
G^*	fractional area participating in ridging	0.15
H^*	determines mean thickness of ridged ice	25 m
C_s	fraction of shear energy contributing to ridging	0.25
C_f	ratio of ridging work to PE change in ridging	17.

an empirical constant β , the ice salinity S , and the temperature T . The salinity profile varies from $S = 0$ at the top surface ($z = 0$) to $S = S_{max}$ at the bottom surface ($z = 1$).

2.2 Dynamics and Ridging Parameters

Ice motion and deformation are determined by balancing five major stresses: wind stress from the atmosphere, water stress from the interaction between ice and ocean, Coriolis force, the stress from the tilt of the ocean surface, and the internal ice stress. A momentum balance equation is solved to obtain the ice velocity in each grid cell, using the elastic-viscous-plastic (EVP) rheology [3] to relate the internal ice stress and the rates of strain. The drag coefficient D_w is used to determine the stress between the ocean and the ice. The ice ridging scheme of the CICE code includes several tuning parameters. An empirical constant G^* is used to determine a ridging weighting function. Larger values of G^* allow thicker ice to participate in ridging, thereby increasing the ice strength. H^* determines the thickness of ridging ice. C_s is the fraction of shear dissipation energy that contributes to ridge building. Another empirical parameter, C_f , accounts for frictional energy dissipation.

3 Processing the CICE Code with TAPENADE

Given the Fortran 90 CICE code, TAPENADE successfully produced a portable Fortran 90 CICE.AD code that allows the tangent linear derivative computation

of partial derivatives of ice conditions with respect to various thermodynamic and dynamic input parameters. Still under the development, TAPENADE supports most of the Fortran 90 standard. Lack of support for `count`, `present`, and dynamic memory allocation requires a preprocessing step to replace some Fortran 90 constructs with ones acceptable to TAPENADE. Also, some type mismatch problems with the Fortran `MOD` intrinsic function calls were observed in processing the CICE code. Various `netCDF` calls are used in the CICE code to write a restart file and history files during simulation. Working as I/O statements, these `netCDF` routines are not directly related to the differentiation process. We used TAPENADE's blackbox approach to bypass the `netCDF` routines when differentiating. To do this, we had to supply differentiation information to TAPENADE. The same approach was used to handle the MPI library routine calls in the CICE code. The number of lines of the TAPENADE-generated CICE code (50000 lines) is about double the size of the original CICE code (27000 lines). The computational time of the AD-generated tangent-linear CICE code increased proportionally with the number of independent variables.

4 Numerical Results

4.1 Valid Derivative Computation with Pre-tuning Step

In the EVP ice dynamics of the CICE model, several tuning parameters are used to maintain the stability of the EVP routine. The constraining constant Δ_{min} (named *tinyarea*) for the ice strain rate computation $P/\max(\Delta, \Delta_{min})$ critically controls the convergence behavior of computed ice velocity. Figure 1 shows the ice velocity computation with different values of *tinyareas* for the EVP subcycling iterations. In the figure, the AD-generated derivatives are also plotted for each of the choices of *tinyarea*. The derivatives are computed for the ice velocity with respect to the ocean drag coefficient. Significant oscillations were observed in ice velocity computation with the smaller value of *tinyarea*, which resulted into a divergent behavior of the AD-generated derivatives. Thus, we further tuned the CICE code with increased *tinyarea* to maintain the stability of the AD-generated derivatives. Similar oscillations were reported by Bücker [1] with two-dimensional aircraft design optimization problems. They used delayed propagation approach to control the oscillation.

4.2 AD Sensitivity Experiment

Two different problem sets were used for the sensitivity experiments: 100×116 and 900×601 orthogonal grid points with 5 different ice categories and 4 ice layers in single ice category. The forcing variables of surface air temperature, specific humidity, down-welling short-wave and long-wave radiation, and geostrophic winds derived from National Centers of Environmental Prediction (NCEP) reanalysis and European Center for Medium-Range Weather Forecasts (ECMWF) global analyses were used for the simulation of the year 1987 and 1996. The multi-year spin-up result of ice thickness, concentration, and velocity

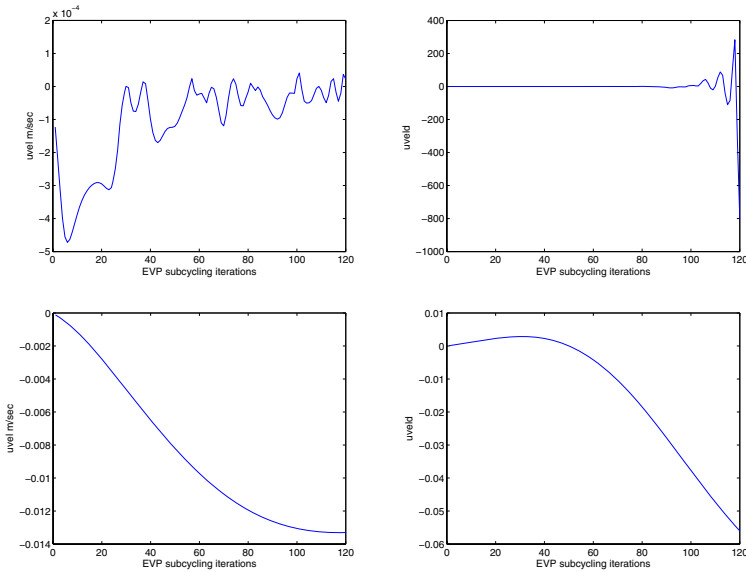


Fig. 1. Convergence behaviors of EVP subcycling step: a) u -velocity computed with $tinyarea = 1. \times 10^{-12}$, b) its AD derivative with $tinyarea = 1. \times 10^{-12}$, c) u -velocity computed with $tinyarea = 1. \times 10^{-6}$, and d) its AD derivative with $tinyarea = 1. \times 10^{-6}$

fields on January 1 was used as the initial state for the experiments. Sensitivity experiments were carried out with respect to two main dependent variables, ice thickness and hemispheric ice volume. A linux cluster system was used to run the numerical experiments. Table 2 shows the measured parallel performance of the CICE.AD code. Reasonable speed-up was achieved on up to 60 processors. Most of the computational time was spent on the ice dynamic part where the momentum equations for ice velocity are explicitly integrated.

Table 3 shows the sensitivity results of hemispheric ice volume for the 1987 ice conditions on coarse grid data. Note that the ice volume can be directly computed by the multiplication of ice thickness and area of each grid cell. The derivative numbers were nondimensionalized by using the computed ice volume and parameter values. The first column of the table lists the 12-month sum of sensitivity magnitudes for each of the 20 parameters, with larger values indicating greater sensitivity. The high sensitivity result of ice density is largely an artifact of the way density is treated in the CICE code. Increasing ice density resulted in a smaller value of the specific heat of melting and a higher temperature change. This unphysical warming reduces winter ice growth and increases summer melting. Multiple year runs are required to determine the true sensitivity of the thickness to ice density. From the table we see that parameters affecting the conductivity and radiative absorption are of paramount importance for simulating ice volume in the sea ice model; with the exception of D_w , dynamics and ridging parameters are less important than the thermodynamic parameters. If we were using ice velocity as the dependent variable, however, the dynamics

Table 2. Computational time (seconds) of the CICE.AD code for the fine grid problem set: multi-directional tangent derivative computation for one-day (January 1 of 1996) sensitivity computation of two independent parameters, ρ_i and α_{iv}

Routines	10 CPUs	20 CPUs	30 CPUs	60 CPUs
Total	1256.02	772.70	493.70	314.91
Dynamics	829.32	511.24	338.87	200.03
Advection	184.06	96.74	66.33	37.15
Thermo	93.00	42.78	26.67	11.95
Ridging	15.80	7.52	5.24	2.53
Cat Conv	12.84	5.66	3.84	1.62
Bound	701.79	444.91	291.25	173.64

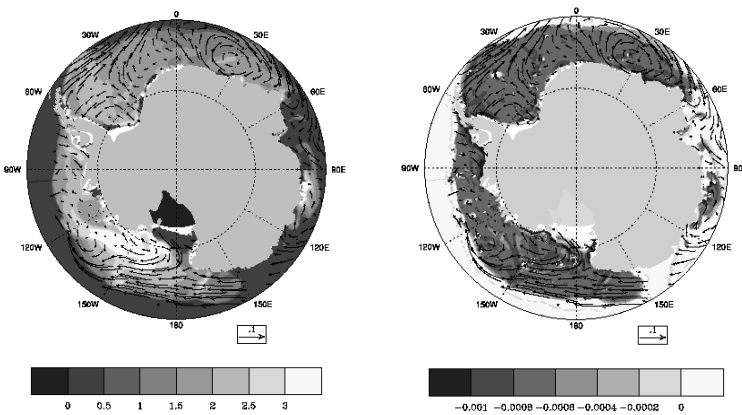


Fig. 2. Ice thickness (m) distribution of the first week of January, 1996 (*left*) and colormap of sensitivity to ice density (*right*): 900×601 orthogonal grid points

parameters would be more prominent. For the fine grid problem, Figure 2 shows the sensitivity distribution of ice thickness to ice density over Antarctic region. The derivative colormap shows how the ice density affects on the ice thickness computation.

5 Summary

In this study, a sensitivity-enhanced simulation approach for global sea-ice modeling was investigated through the AD method. We observed a pre-tuning step was required to obtain stable convergence behaviors of the AD-based CICE code. An important result from this study is the prominent sensitivity of ice thickness to radiative control parameters. For example, emissivity and albedo parameters have not been scrutinized in sea ice model development. This study shows that multivariate sensitivity analysis for those parameters can be easily accomplished based on the AD method. Also, the AD-based scheme for computing derivatives provides an efficient guideline to adjust those important parameters.

Table 3. Magnitudes of AD sensitivities, summed over the 12 months for northern hemisphere ice volume and its monthly sensitivity for the year of 1987

Parameter	sum	January	April	July
ϵ	0.6439×10^{-1}	0.1057×10^{-2}	0.1497×10^{-2}	0.2075×10^{-1}
u_{min}	0.4450×10^{-3}	0.4061×10^{-4}	0.1133×10^{-4}	-0.6007×10^{-5}
α_{iv}	0.1088	0.8533×10^{-4}	0.2259×10^{-2}	0.3200×10^{-1}
α_{in}	0.1057	0.2317×10^{-4}	0.7777×10^{-3}	0.3573×10^{-1}
α_{sv}	0.2050×10^{-1}	0.2577×10^{-3}	0.3578×10^{-2}	0.8714×10^{-3}
α_{sn}	0.1184×10^{-1}	0.9199×10^{-4}	0.1494×10^{-2}	0.9106×10^{-3}
i_c	0.2079×10^{-1}	-0.3489×10^{-4}	-0.3462×10^{-3}	0.7601×10^{-2}
κ_i	0.3247×10^{-2}	-0.3503×10^{-5}	0.3237×10^{-4}	0.1125×10^{-2}
ρ_i	$0.2044 \times 10^{+1}$	-0.2759	-0.1782	-0.7975×10^{-1}
β	0.1092×10^{-1}	-0.1625×10^{-2}	-0.1031×10^{-2}	-0.1974×10^{-3}
k_o	0.1796	0.2809×10^{-1}	0.1537×10^{-1}	0.1432×10^{-2}
ρ_s	0.2784×10^{-1}	0.2191×10^{-2}	0.5501×10^{-2}	0.6088×10^{-4}
k_s	0.5190×10^{-1}	0.1034×10^{-1}	0.1944×10^{-2}	0.3975×10^{-4}
S_{max}	0.1161	0.1114×10^{-1}	0.1012×10^{-1}	0.9196×10^{-2}
h_{mix}	0.4713×10^{-1}	-0.5548×10^{-2}	-0.2656×10^{-2}	0.4201×10^{-2}
D_w	0.4723×10^{-2}	-0.6713×10^{-3}	-0.4030×10^{-4}	0.2838×10^{-4}
G^*	0.2742×10^{-2}	0.2370×10^{-3}	0.1088×10^{-3}	-0.3818×10^{-3}
H^*	0.1233×10^{-2}	-0.2690×10^{-3}	-0.1638×10^{-3}	0.1209×10^{-4}
C_s	0.3252×10^{-2}	0.5369×10^{-3}	0.3284×10^{-3}	-0.3460×10^{-4}
C_f	0.3526×10^{-2}	-0.6684×10^{-3}	-0.4144×10^{-3}	0.5138×10^{-4}

Implemented by the black-box approach of TAPENADE, the parallel MPI routines of the CICE were successfully processed. Significant parallel performance was obtained for a large-size problem set. In future work, we plan to further explore the CICE model’s parameter space using the best available data for both hemispheres, including satellite-derived ice concentration and ice deformation. Furthermore, we plan to tune the model using long-term (decadal) observational data.

Acknowledgement

This work was supported by the Climate Change Research Division subprogram of the Office of Biological & Environmental Research, Office of Science, U.S. Department of Energy through the Climate Change Prediction Program (CCPP), and the Scientific Discovery through Advanced Computing (SciDAC) Program under Contract W-31-109-ENG-38.

References

1. H. M. Bücker, A. Rasch, E. Slusanschi, and C. H. Bischof, *Delayed Propagation of Derivatives in a Two-dimensional Aircraft Design Optimization Problem*, Proceedings of the 17th Annual International Symposium on High Performance Computing Systems and Applications and OSCAR Symposium, Sherbrooke, Québec, Canada, May 11–14, 2003, NRC Research Press, 2003.

2. M. Harder and H. Fischer, *Sea ice dynamics in the Weddell Sea simulation with an optimized model*. J. Geophys. Res., 104: 11,151–11,162, 1999.
3. E. C. Hunke and W. H. Lipscomb, *CICE: the Los Alamos Sea Ice Model, Documentation and Software*, LA-CC-98-16, Los Alamos National Laboratory, NM, 2004.
4. L. Hascoet and V. Pascual, *TAPENADE 2.1 User's Guide, INRIA Technical Report*, <http://www-sop.inria.fr/tropics>, 2004.
5. P. A. Miller, S. W. Laxon, D. L. Feltham, and D. J. Cresswell, *Optimization of a sea ice model using basin-wide observations of Arctic sea ice thickness, extent and velocity*, J. Clim., 2005 (in press).
6. C. L. Parkinson and W. M. Washington, *A large-scale numerical model of sea ice*, J. Geophys. Res., 84:311–337, 1979.